Carbohydrate Polymers 87 (2012) 2154–2159

Contents lists available at SciVerse ScienceDirect

Carbohydrate Polymers

journal homepage: www.elsevier.com/locate/carbpol

Characterization of hydroxyl groups of highly crystalline β-chitin under static tension detected by FT-IR

Yukie Saito*, Tadahisa Iwata

Graduate School of Agricultural and Life Sciences, The University of Tokyo, 1-1-1 Yayoi, Bunkyo-ku, Tokyo 113-8657, Japan

ARTICLE INFO

Article history:
Received 6 August 2011
Received in revised form 10 October 2011
Accepted 17 October 2011
Available online 18 November 2011

Keywords:
β-Chitin
Hydrogen bonding
Deuteration
FT-IR under static tension

ABSTRACT

The different behavior of the OH groups of a highly crystalline β-chitin from *Lamellibrachia* sp. was revealed by FT-IR spectroscopy with static tension applied in the direction of the chain. Both OH groups shifted to higher wavenumbers under the tension, possibly because the force constant of the OH vibration intensified due to the erosion of hydrogen bonds, but the shift in the OH peak occurring at 3435 cm^{-1} was 14% greater than that of the peak at 3470 cm^{-1}. The band at 3435 cm^{-1} was assigned to O(3)H and that at 3470 cm^{-1} to O(6)H, because the intramolecular hydrogen bond of O(3)H···O(5) occurs along the chitin chain's backbone and is likely to be more affected under tensile stress as a load carrier, than O(6)H···O(7)═C, which is an intermolecular hydrogen bond located in a branch of the chain. Computation of an IR spectrum under stretching was conducted and supported the assignment of the two OH groups.
© 2011 Elsevier Ltd. All rights reserved.

1. Introduction

Chitin, poly [β (1→4)-2-acetamido-2-deoxy-D-glucopyranose], is a linear polysaccharide and after cellulose the most abundant biopolymer on earth. Its *N*-acetyl amide groups can be chemically altered to derive compounds, such as chitosan, that are used in chemical, medical, and industrial fields. Chitin has at least two naturally occurring crystalline polymorphs (Rudall & Kenchington, 1973). One form is α-chitin, where two antiparallel chains are packed into a unit cell (Minke & Blackwell, 1978), which occurs in the cuticles of insects or the exoskeletons of crustaceans. The other form is β-chitin, which consists of parallel chains (Gardner & Blackwell, 1975), and is found in squid pens, the spines of some diatoms, and the tubes of some pogonophorans and vestimentiferans. Whereas α-chitin is stable, β-chitin has the unique property of accepting small molecules as intercalates within its crystalline lattice, such as in β-chitin hydrate (Blackwell, 1969), yielding a series of crystallosolvates in the form of lamellar compounds (Saito, Okano, Putaux, Gaill, & Chanzy, 1997; Saito, Okano, Gaill, Chanzy, & Putaux, 2000, Saito, Tomotake, & Shida, 2007). This quasi-stable crystalline feature of β-chitin is expected to aid the development of new composite materials having, for example, molecular-scale sandwich structures. For designing materials, knowledge of the role of the two OH groups in β-chitin is important, as they can influence a reaction process or the resulting properties of the derivatives.

IR spectroscopy is a powerful tool for characterizing OH bands. In the case of cellulose, poly [β (1→4)-D-glucopyranose], a difference in the accessibility of its three OH groups was revealed (Kondo, 1994, 1997). For α-chitin, there are three OH absorption bands with different energy levels that can be explicitly assigned using two-dimensional FT-IR methods (Yamaguchi, Nge, Takemura, Hori, & Ono, 2005). On the other hand, there have been several reports on β-chitin (Blackwell, Parker, & Rudall, 1967; Falk, Smith, McLachlan, & McInnes, 1966; Focher, Naggi, Torri, Cosani, & Terbojevich, 1992; Gow, Gooday, Russell, & Wilson, 1987; Kim, Kim, & Lee, 1996) derived from squid pens or diatom spines, and the OH region has not been discussed or assigned precisely so far. This may be partly because squid pen chitin, frequently used as a source of β-chitin, has disordered structural features that lead to a single broadened OH band centered at around 3444 cm^{-1} (Focher et al., 1992). In this study, highly crystalline β-chitin from a vestimentiferan tube was used, and the OH band was resolved into individual peaks and characterized using FT-IR spectroscopy.

To elicit the difference between and assign the two OH groups of β-chitin, FT-IR was conducted while the highly crystalline sample was statically stretched in the direction of the chitin chain. The β-chitin crystal has two OH groups, O(3)H, forming an intramolecular hydrogen bond with O(5), and the O(6)H, forming an intermolecular hydrogen bond with C═O(7′) of the next chain, according to the model proposed by Gardner and Blackwell (Fig. 1) (Gardner & Blackwell, 1975). There have been several reports that load-carrying atomic bonds can be influenced by dynamic or static stress, with a resulting shift in wavenumber (Wu, Tashiro, & Kobayashi, 1989; Bowden, Gardiner, & Southall, 1993; Rdriguez-Cabello, Merion, Jawhari, & Pastor, 1995). In this study, we tried to

* Corresponding author. Tel.: +81 3 5841 5246; fax: +81 3 5841 5246.
E-mail addresses: aysaito@mail.ecc.u-tokyo.ac.jp (Y. Saito), atiwata@mail.ecc.u-tokyo.ac.jp (T. Iwata).

0144-8617/$ – see front matter © 2011 Elsevier Ltd. All rights reserved.
doi:10.1016/j.carbpol.2011.10.044

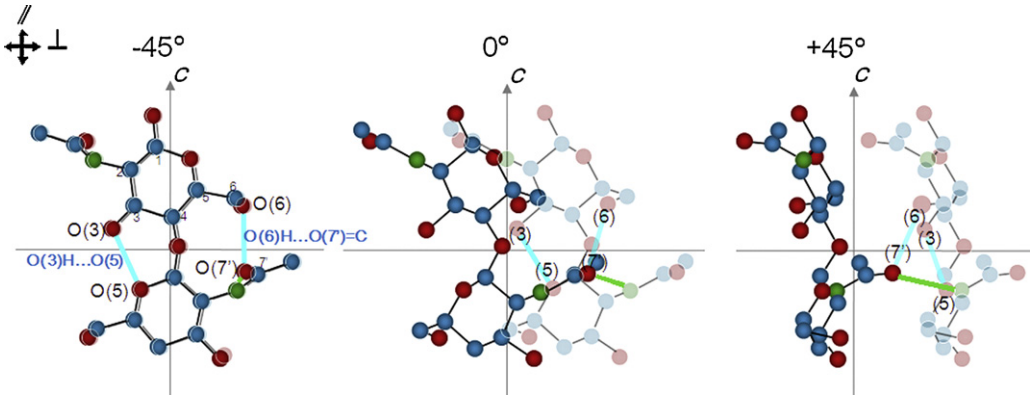

Fig. 1. Projections of the Cartesian coordinates of the β-chitin crystal model of Gardner and Blackwell (1975). A chain is represented by two residues. Two chains are plotted, with the chain at the back shown as faded. Lines in pale blue = the hydrogen bond of O(3)H···O(5) (intramolecular) and hydrogen bond of O(6)H···O(7′)═C (intermolecular). Lines in green = the amide hydrogen bond of NH···O(7′)═C (intermolecular). Balls in blue = carbon, red = oxygen, and green = nitrogen.

assign two OH groups of the β-chitin crystal based on the differences in the shifts. Beside static tensile FT-IR measurements, the computation of an IR spectrum under stretching using Cerius^2 was supplementarily conducted.

2. Experimental

2.1. Preparation of the β-chitin sample

β-Chitin from the tubes of *Lamellibrachia* sp. was used. The tubes resemble those of *Tevnia* sp., a kind of vestimentiferan, and consisted of chitin ribbons ranging in thickness from 0.1 to 1 μm (Gaill, Persson, Sugiyama, Vuong, & Chanzy, 1992). Each ribbon was assembled in a random twisted nematic form, consisting of highly crystalline β-chitin microfibrils stacked in an approximately axial orientation, filled with a protein matrix (Gaill et al., 1992). The *Lamellibrachia* sp. tubes were deproteinized according to the method of Gaill et al. (1992) to obtain an axially oriented β-chitin sample with the original orientation. No protein peaks were detected in FT-IR spectra after this treatment. Pieces of purified *Lamellibrachia* tubes were carefully delaminated using tweezers in tap water and sheet samples <50-μm thick with the original orientation were obtained. They were then dried on Teflon plates at 105 °C overnight to remove all moisture. To examine the orientation of this sample, X-ray diffraction was applied using Ni-filtered Cu Kα radiation (λ = 0.15418 nm) employing a Rigaku X-ray generator operating at 50 kV and 100 mA with a vacuum camera. The diffraction patterns were recorded on Fuji imaging plates. Fig. 2 is a diffractogram of the sample. In the diffractogram with the reflections tangentially streaked, the orientation of β-chitin microcrystals has a slight distribution but is axially orientated.

2.2. Deuteration of the β-chitin sample

The purified and dried β-chitin sample was immersed in D_2O at room temperature for a period of 2 h then dried at 105 °C overnight. This treatment caused intracrystalline swelling and the OH groups in the crystalline regions were successfully converted to OD, since liquid D_2O readily intercalated between the chitin molecular sheet arrangement along the *ac* plane of crystalline β-chitin, where substitution of the OH group by an OD group occurs with ease (Saito et al., 2000).

2.3. FT-IR measurements

The IR measurements were performed using a Nicolet Magna 860 FT-IR spectrometer. All spectra were recorded in the transmission mode with a resolution of 2 cm^{-1} under flowing dry N_2 gas to alleviate the noise caused by H_2O in the air. The polarization FT-IR spectroscopy was carried out using a ZnSe wire grid polarizer located in front of the sample.

For the measurements under static tension, both ends of the samples were held in a stretcher equipped with a micrometer, a pressure gauge and a data logger. The samples were stretched at the micron scale by the modified micrometer attached to a clamp and the apparent stress was calculated from the tensile stress value of the pressure gauge divided by the cross-sectional area of the sample plane perpendicular to the direction of tension. The positions of almost of all peaks shown in Table 1 were measured by reading the wavenumbers that gave the local maximum values. However regarding the major absorption bands of two OH groups, NH group, OD groups, C═O group, bridge C–O–C, the peak positions were measured with the spectra baseline-corrected by drawing straight lines between 3375 and 3504, 3225 and 3350, 2480 and 2600, 1485 and 1700, 985 and 1185 cm^{-1}, respectively, and by curve-fitting for the mixture of Gaussian and Lorentzian line by "PeakSolve" program in Garactic Industries Corporation.

2.4. Computation of the IR spectra using Cerius^2

The IR spectrum of a β-chitin crystal under tensile stress was simulated using the Cerius^2 software package (Molecular Simulations Inc., San Diego, distributed by Ryoka Systems Inc.,

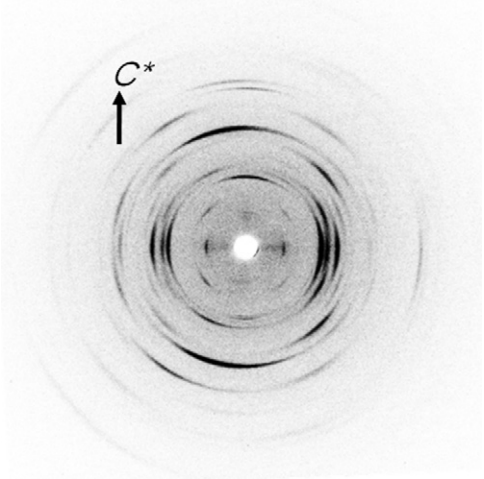

Fig. 2. X-ray diffractogram of *Lamellibrachia* β-chitin samples.

Table 1
IR bands of *Lamellibrachia* β-chitin and their shifts under a tensile stress of 0.22×10^{-5} GPa along the chain. The orientation was determined by polarization FT-IR without tension.

Absorption frequency (cm^{-1})			Orientation	Assignment
Band position		Shift amount		
Unloaded	Under tensile stress	Under tensile stress		
3470.8	3474.0	3.2	//	OH St
3435.0	3438.5	3.5	//	OH St
3292.9	3292.8	−0.1	⊥	NH St
2914.3	2915.2	1.0	⊥	CH_x region. . .?
2868.7	2867.7	−1.0	⊥	CH St[a]
2829.5	2826.9	−2.6	?	CH_2 sym. St[a]
1629.8	1629.8	0.0	⊥	C=O St (Amide I)
1556.7	1556.7	0.0	⊥	NH Bn (Amide II)
1455.6	1455.7	0.1	⊥	
1431.4	1431.5	0.1	⊥	CH_2 Bn and CH_3 Df[a]
1380.1	1380.5	0.4	⊥	CH Bn and CH_3 sym Df[a]
1373.1	1372.1	−1.0	//	
1363.2	1361.6	−1.6	⊥	
1329.5	1329.0	−0.4	//	
1321.1	1318.7	−2.4	//	
1311.9	1310.3	−1.6	⊥	Amide III and CH_2 wagging[a]
1303.1	1301.6	−1.6	⊥	
1266.2	1265.7	−0.6	⊥	
1245.3	1243.9	−1.4	⊥	
1200.4	1199.5	−0.9		
1152.7	1150.1	−2.5	//	Assym bridge C–O–C St[a]
1136.7	1136.2	−0.5	//	
1121.9	1120.4	−1.4	⊥	
1109.4	1108.0	−1.4	//	
1103.3	1100.4	−2.9	//	
1078.0	1074.7	−3.3	⊥	
1062.6	1060.6	−2.1	//	C–O St
1040.8	1040.2	−0.6	//	
1025.5	1024.4	−1.1	//	
991.2	990.3	−0.9	⊥	
970.8	967.4	−3.4	//	CH_3 wagging along chain[a1]
954.4	953.9	−0.5	⊥	
924.7	923.9	−0.7	?	
890.4	888.0	−2.3	//	Ring St?[a]

[a] The assignment refers to that of α-chitin (Pearson, Marchessault, & Liang, 1960).

Japan). For this purpose, an initial β-chitin crystal model was built based on the fractional coordinates of Gardner and Blackwell (1975), using a periodic model with space group P1. Then, this modeled β-chitin crystal unit was extended along the *c*-axis direction by 1%. Energy minimization calculations were carried out using the CFF91 force field, where all the relevant degrees like quartic bond and bond angles contributions are free, three first Fourier components for dihedral angles and all the cross contributions between intra-molecular degrees are free. CFF91 is useful for small models of gas-phase geometries, vibrational frequencies, conformational energies, torsion barriers, crystal structures of hydrocarbons and protein–ligand interactions. It is extensively applied in the structural optimization of hydrocarbons and their derivatives, including carbohydrates (Shimada, Kaneko, Takada, Kitamura, & Kajiwara, 2000; Melani et al., 2003). The optimized model under extension was used for the computation of the IR spectra using Cerius[2].

3. Results

3.1. FT-IR spectroscopy under static tension

Very sharp IR spectrograms were obtained from the highly crystalline β-chitin of *Lamellibrachia* tubes (Fig. 3). The spectrograms are typical for β-chitin, having a single C=O band at 1630 cm^{-1} due to the bifurcated hydrogen-bond between C=O(7) and N–H (intermolecular) and O(6)H (intramolecular), as shown in Fig. 1. Fig. 3 shows the slight trace of a shoulder at around 1653 cm^{-1}, which can appear even in highly crystalline samples and probably arises from disordered areas on the surface of the crystal (Saito et al., 2000), where the hydrogen-bond of C=O is not bifurcated. The highly crystalline β-chitin sample was stretched along the chain and the sample in the stretched state was subjected to FT-IR spectroscopy (Fig. 3a and b). Table 1 indicates the shifts under tensile stress, and whether each band appears stronger with parallel or perpendicular polarization along the chain's axis. Nearly half of the parallel bands showed a shift of more than 1 cm^{-1}, while only one quarter of the perpendicular bands did. The bands parallel to the direction of tensile stress probably have a tendency to shift more than do the perpendicular bands. In Fig. 3c, secondary derivatives of absorbance of typical parallel bands (OH and bridge C–O–C) and perpendicular bands (C=O and NH) are shown. The parallel bands changed severely by the stress, but the perpendicular bands unchanged. The curve fitting of the formers clearly shows the change of peak position under a tensile stress. In Fig. 4, absorbance of them is plotted versus the various level of tensile stress applied along the length of the chain. As the level of stress increased, the shifts of the bands at 3470 and 3435 cm^{-1} of the two OHs and at 1153 cm^{-1} of C–O–C increased linearly, while the bands at 3293 cm^{-1} of NH and at 1630 cm^{-1} of C=O were essentially unchanged. According to the crystal model of Gardner and Blackwell (1975), the directions of the O(3)H, O(6)H and bridge C–O–C bonds are aligned close to the chain direction (Fig. 1) and they possibly have a load-bearing function under tensile stress along the chain. On the other hand, the NH and C=O(7) bonds are aligned almost perpendicular to the direction of tensile stress. In addition, they interacted via extremely strong amide hydrogen bonds (Saito et al., 2000) which might stabilize their position even under tensile stress.

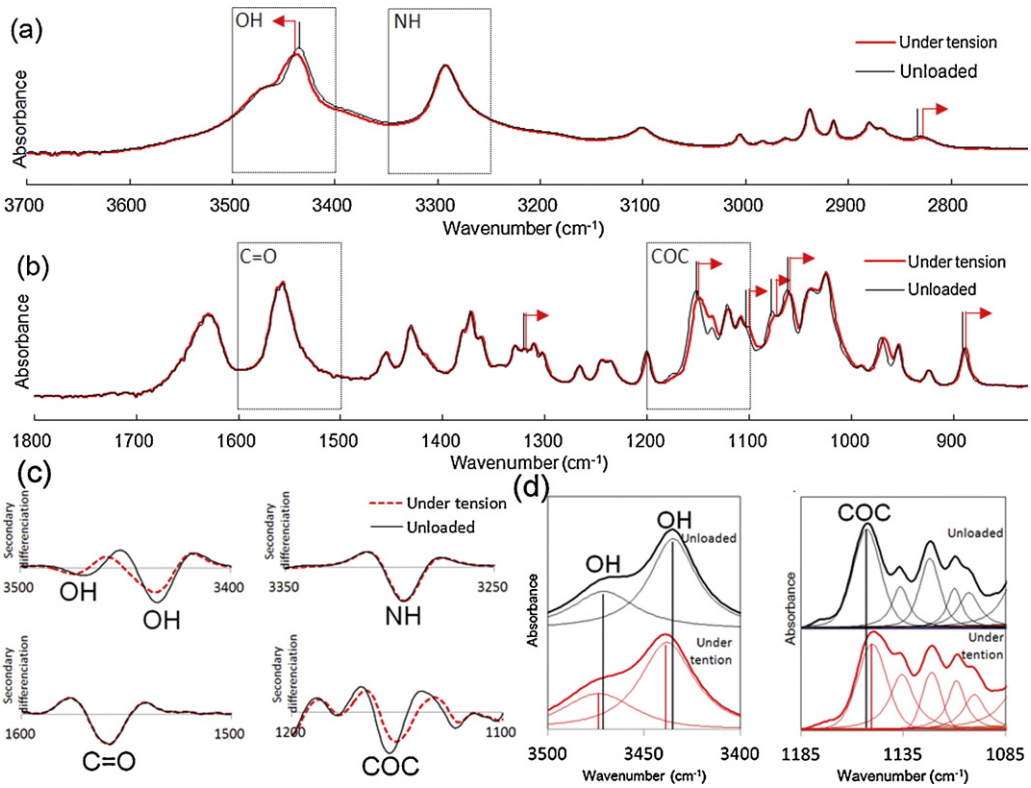

Fig. 3. FT-IR spectrum of a *Lamellibrachia* β-chitin sample under a tensile stress of 0.22×10^{-5} GPa along the chain: (a) 3700–2700 cm^{-1} and (b) 1800–800 cm^{-1} regions. (c) second differentiations and (d) curve fittings of the major groups insets.

The shift in IR bands under static tension can be interpreted theoretically as follows. According to the normal vibration principle, the wavenumber $\tilde{\nu}_{AB}$ of a stretching vibration of a bond between atom A and atom B is expressed by the well-known equation:

$$\tilde{\nu}_{AB} = \frac{1}{2\pi c} \cdot \left(\frac{k_{AB}}{M_A M_B / (M_A + M_B)} \right)^{1/2}$$

where c is the velocity of light, k_{AB} is the force constant of bonding, and M_A and M_B are masses of the two atoms. This equation means that $\tilde{\nu}_{AB}$ increases with the value of k_{AB}. When a bond distance is lengthened, such as by tensile force, in general, k_{AB} is expected to be weakened and consequently $\tilde{\nu}_{AB}$ decreases. This explains why almost all the parallel stretching bands shifted to a lower wavenumber when the tensile stress was applied along the chain (Table 1), as shown by the bridge C–O–C band occurring at 1153 cm^{-1} (Fig. 4, right). In contrast, the two OH bands shifted to higher wavenumber following tensile stress (Fig. 4, left). This shift can be explained as follows. If we assume that Atom B forms a hydrogen bond with another atom, Atom C, resulting in A–B···C, then if tensile force acts in the direction of AC, the distance between A and C increases. Then, the hydrogen bond B···C must be weakened and the covalent bond A–B must strengthen as a consequence. As a result, the value of k_{AB} increases and this increases the value of $\tilde{\nu}_{AB}$.

The difference in the shift of the two OH groups observed in Fig. 4 may reflect environmental influences. Considering the molecular frame of chitin, the assignments of the two OH groups were deducted as follows: the hydrogen bond O(3)–H···O(5) would be more severely affected by tensile stress along the chain than would O(6)H···O(7′)=C. In O(3)–H···O(5), the O(5) is a member of the main chain and O(3) is mediated by 1 bond to the main chain; that is, both of these atoms are positioned on the load-carrying backbone (Fig. 1). Meanwhile, the O(6) atom is connected by 2 bonds to the main chain and the O(7′) atom is connected by 3 bonds located far from the main chain. Compared to O(3)H···O(5), O(6)H···O(7′)=C is located far from the main chain and the bonds possibly allow conformational changes, which may release the stress on the hydrogen bond. As a result, the distance between O(6) and O(7′) is possibly not distorted as much by tensile stress as the distance between O(3) and O(5), and so the shift in wavenumber of O(6)H is expected to be less than that of O(3)H. As shown in Fig. 4, the shift in the OH band at 3435 cm^{-1} was 14% greater than that of the band at 3470 cm^{-1}. This may suggest that the two bands can be assigned to the O(3)H and O(6)H groups, respectively.

This hypothesis was examined also by the measurement of the substituted OD stretching region. Deuteration measurements have two advantages. The first is that tracing using OD is a sure method for investigating crystalline hydrogen groups. The OH region can be overlapped by absorbed H_2O from the ambient air, which could easily enter into the sample chamber during the measurements, even under flowing dry N_2 gas. Also the moisture probably generated free OH on the surface of the crystallites, though it should be expected to be small amount due to the almost perfect crystallinity of the sample. Gaseous H_2O from the ambient air is not able to penetrate the β-chitin crystal during the short time scale of this IR measurement, and the crystalline OD of the deuterated sample is maintained without being substituted by OH. Thus, measuring the OD region is a reliable way of observing genuine crystalline hydroxyl groups. The second advantage is that the OD region does not overlap with the background signals of ambient H_2O and CO_2. For sequential FT-IR measurements with incremental steps in tensile stress, it takes several minutes for each step to obtain the spectra, and then a mismatch in the background can happen, especially toward the end step of the measurement. This effect does not occur in the OD region, and thus each band could be observed more clearly. In the spectrum of the deuterated samples, crystalline OD bands occurred at 2570 and 2544 cm^{-1}. They correspond to the

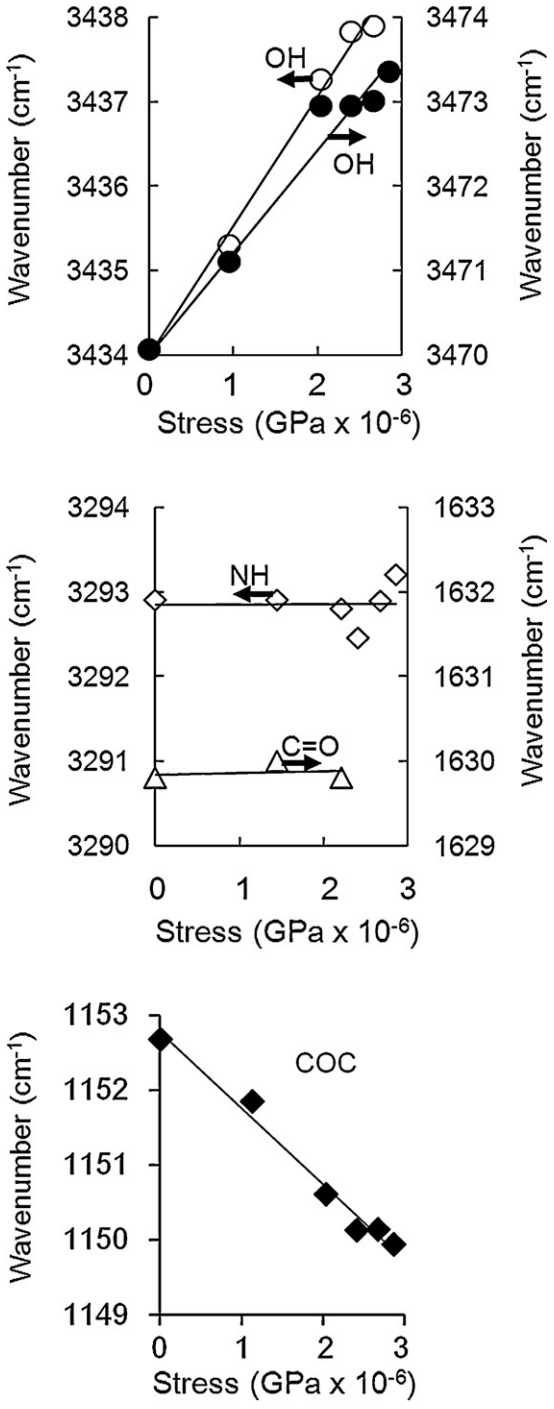

Fig. 4. Change in the position of the two OH groups (circles), NH group (open squares), C=O group (triangles), and bridge C–O–C (filled squares) of the FT-IR band vibrational frequencies observed for *Lamellibrachia* β-chitin under tensile stress applied along the chain. The peak for the C=O stretching at a stress >0.24×10^{-5} GPa could not be measured because of the increasing overlap of bands occurring around 1635 cm^{-1} from H_2O absorbed from the ambient air (Kondo, 1997).

original OH bands occurring at 3470 and 3435 cm^{-1}, respectively. The observed shift factors, i.e., the values of the OH group wavenumbers divided by those of the corresponding OD groups, were 1.349 and 1.350. These values are very close to the theoretical shift factor, which was calculated to be 1.34, based on the extra mass of deuterium compared with hydrogen (Jarvis & McCann, 2000). Fig. 5 shows an example of an observed spectrum of the OD stretching region along with the

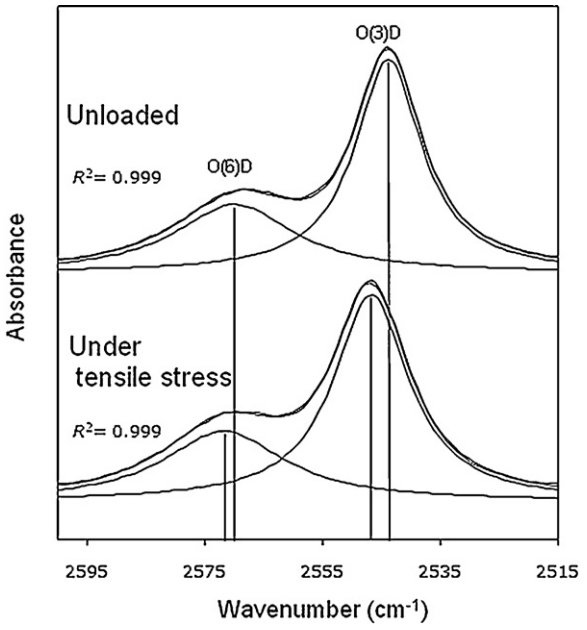

Fig. 5. Curve fitting of the OD stretching regions under a tensile stress of 0.29×10^{-5} GPa for *Lamellibrachia* β-chitin.

associated curve fitting. Under tensile stress, a higher wavenumber shift was also observed with OD bands. Shifts of OD bands produced under stepwise increments in tensile stress were plotted in Fig. 6 and fitted to lines. The increase in the shift of the band occurring at 2544 cm^{-1} was 50% larger than that of the band occurring at 2570 cm^{-1}, which is consistent with the behavior of the parental two OH bands. Thus, the different behavior of the two hydroxyl groups under tensile stress was also confirmed with those deuterated.

3.2. Cerius[2] computation of IR spectrum under static tension

The IR spectrum under static tension was computed using Cerius[2] applied to the atomic coordinates of the β-chitin crystal modeled by Gardner and Blackwell (1975). In the higher wavenumber region (>3300 cm^{-1}), there appeared O(6)H, O(3)H and NH bands occurring at 3563, 3508 and 3413 cm^{-1}, respectively (Fig. 7) and they fitted the observed spectrum quite well, while at lower wavenumbers, further improvement is needed for mal-fits due to disruptions of multiple vibrations. In Fig. 7 the O(6)H band appeared

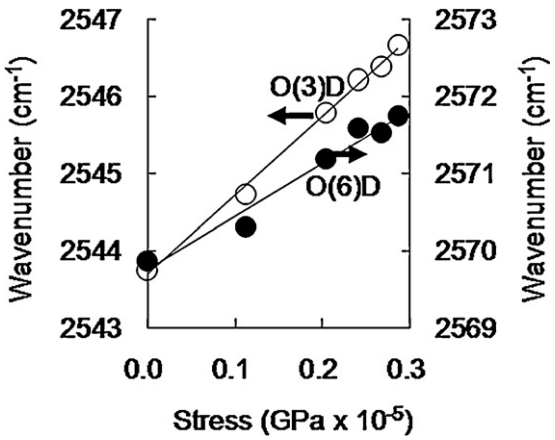

Fig. 6. Change in the position of the OD groups of FT-IR bands observed for *Lamellibrachia* β-chitin under static tension along the chain.

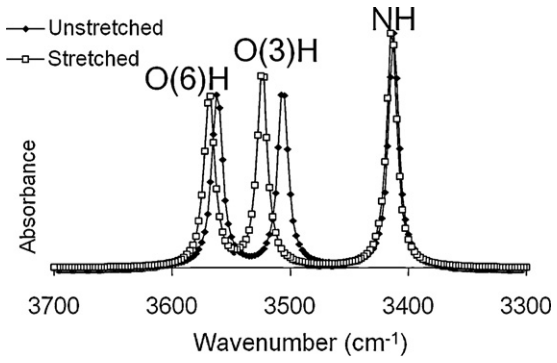

Fig. 7. Cerius[2] simulation of the OH and NH bands of the β-chitin crystal model of Gardner and Blackwell (1975), under stretching along the chain.

at a higher wavenumber than the O(3)H band, which is consistent with the observed results above. With the stretched model along the chain axis, O(6)H and O(3)H bonds moved to higher wavenumbers, appearing at 3569 and 3524 cm^{-1} respectively, while the NH band barely shifted, occurring at 3414 cm^{-1}. The computed shift of O(3)H was three times that of O(6)H.

4. Discussion

Considering all the results, the assignment of the bands occurring at 3470 and 3435 cm^{-1} in crystalline β-chitin is concluded to be O(6)H and O(3)H, respectively. This resembles the case of α-chitin, where the higher wavenumber corresponds to O(6)H and the lower wavenumber corresponds to O(3)H, i.e., the band occurring at 3482 cm^{-1} is assigned to the O(6)H intermolecular hydrogen bond with an adjacent O(6)H group, and the band occurring at 3421 cm^{-1} is assigned to the O(3)H intramolecular hydrogen bond with the O(5) atom (Yamaguchi et al., 2005). α-Chitin has one more OH stretching band in a much lower region, 3380 cm^{-1}, which is thought to be from the O(6)H group arising from bifurcated hydrogen bonds with an adjacent O(6)H group and a C=O group (Yamaguchi et al., 2005). In contrast, in β-chitin, a third OH stretching band was not observed, meaning that the O(6)H groups of β-chitin do not exhibit bifurcated hydrogen bonding. This characteristic of the O(6)H groups depends on crystalline allomorphs and is consistent with the crystalline models of Gardner and Blackwell (1975) for β-chitin.

Here we used the following method for the assignment of unknown bands. The direction and extent of the shift give a clue as to whether the target atom is in a hydrogen bond or located at load-bearing position on the main chain. But it might be possible to detecting stress upon atomic bond by FT-IR spectroscopy. If further study reveals a relation between the shift and the corresponding stress value or distortion value, it will be possible to use a certain bond, like C–O–C, as a stress sensor.

5. Conclusion

Characterization of the two OH groups of the β-chitin crystal was achieved using FT-IR spectroscopy under static tension applied in the direction of the chain. The stretching bands of the OH groups shifted to higher wavenumbers, but the band occurring at 3435 cm^{-1} had a larger shift under tensile stress than did the band occurring at 3470 cm^{-1}.The corresponding deuterated bands also showed similar behavior. Considering the position of the two OH groups upon the chitin chain, O(3)H is expected to be affected by the tensile stress more than O(6)H. Thus the bands occurring at 3470 and 3435 cm^{-1} can be assigned to the O(6)H and O(3)H groups, respectively.

A Cerius[2] computation of the IR spectrum based on model of Gardner and Blackwell supported this assignment, showing that the O(6)H stretching band appeared at 3563 cm^{-1} and the O(3)H stretching band at 3508 cm^{-1}, and under stretching in the chain's direction, the shift was three times larger for the O(3)H stretching band than for the O(6)H stretching band. The results suggested that the 3470 cm^{-1} and 3435 cm^{-1} bands can be assigned to the O(6)H and O(3)H groups, respectively.

Acknowledgements

We thank professor S. Ohta of The Ocean Research Institute, The University of Tokyo, for providing the *Lamellibrachia* tubes. For a part of this study, Yukie Saito was recipient of a grant-in-aid for the Encouragement of Young Scientists (No. 11760220) from the Japanese Society for the Promotion of Science.

References

Blackwell, J. (1969). Structure of β chitin or parallel chain systems of poly-β-(1-4)-*N*-acetyl-D-glucosamine. *Biopolymers*, *7*, 281–298.
Blackwell, J., Parker, K. D., & Rudall, K. M. (1967). Chitin fibres of diatoms *Thalassiosira fluviatilis* and *Cyclotella cryptica*. *Journal of Molecular Biology*, *28*, 383–385.
Bowden, M., Gardiner, D. J., & Southall, J. M. (1993). Determination of bandshifts as a function of strain in carbon-fibers using Raman-microline-focus-spectrometry (MIFS). *Carbon*, *31*, 1057–1060.
Falk, M., Smith, D. G., McLachlan, J., & McInnes, A. G. (1966). Studies on chitan (β-(1-4)-linked 2-acetamido-2-deoxy-D-glucan) fibers of diatom *Thalassiosira fluviatilis* Hustedt. *Canadian Journal of Chemistry*, *44*, 2269–2281.
Focher, B., Naggi, A., Torri, G., Cosani, A., & Terbojevich, M. (1992). Structural differences between chitin polymorphs and their precipitates from solutions – Evidence from CP-MAS C-13-NMR, FT-IR and FT-Raman spectroscopy. *Carbohydrate Polymers*, *17*, 97–102.
Gaill, F., Persson, J., Sugiyama, J., Vuong, R., & Chanzy, H. (1992). The chitin system in the tubes of deep-sea hydrothermal vent worms. *Journal of Structural Biology*, *109*, 116–128.
Gardner, K. H., & Blackwell, J. (1975). Refiment of structure of β-chitin. *Biopolymers*, *14*, 1581–1595.
Gow, N. A. R., Gooday, G. W., Russell, J. D., & Wilson, M. J. (1987). Infrared and X-ray-diffraction data on chitins of variable structure. *Carbohydrate Research*, *165*, 105–110.
Jarvis, M. C., & McCann, M. C. (2000). Macromolecular biophysics of the plant cell wall: Concepts and methodology. *Plant Physiology and Biochemistry*, *38*, 1–13.
Kim, S. S., Kim, S. H., & Lee, Y. M. (1996). Preparation, characterization, and properties of β-chitin and *N*-acetylated β-chitin. *Journal of Polymer Science Part B: Polymer Physics*, *34*, 2367–2374.
Kondo, T. (1994). Hydrogen bonds in ragioselectively substituted cellulose derivatives. *Journal of Polymer Science Part B: Polymer Physics*, *32*, 1229–1236.
Kondo, T. (1997). The assignment of IR absorption bands due to free hydroxyl groups in cellulose. *Cellulose*, *4*, 281–292.
Melani, F., Mura, P., Adamo, M., Maestrelli, F., Gratteri, P., & Bonaccini, C. (2003). New docking CFF91 parameters specific for cyclodextrin inclusion complexes. *Chemical Physics Letters*, *370*, 280–292.
Minke, R., & Blackwell, J. (1978). Structure of α chitin. *Journal of Molecular Biology*, *120*, 167–181.
Pearson, F. G., Marchessault, R. H., & Liang, C. Y. (1960). Infrared spectra of crystalline polysaccharides. 5. Chitin. *Journal of Polymer Science*, *40*, 101–116.
Rdriguez-Cabello, J. C., Merion, J. C., Jawhari, T., & Pastor, J. M. (1995). Rheooptical Raman-study of chain deformation in uniaxially stretched bulk polyethylene. *Polymer*, *36*, 4233–4238.
Rudall, K. M., & Kenchington, W. (1973). Chitin system. *Biological Reviews*, *49*, 597–636.
Saito, Y., Okano, T., Putaux, J. L., Gaill, F., & Chanzy, H. (1997). In A. Domard, G. Roberts, & K. M. Vårum (Eds.), *Seventh ICCC Advances in chitin science* (pp. 507–512). Lyon: Jacque André Publisher.
Saito, Y., Okano, T., Gaill, F., Chanzy, H., & Putaux, J. L. (2000). Structural data on the intra-crystalline swelling of β-chitin. *International Journal of Biological Macromolecules*, *28*, 81–88.
Saito, Y., Tomotake, Y., & Shida, S. (2007). Formation of a lamellar compound by reaction of acrylic acid crystallosolvated in highly crystalline α-chitin. *Biomacromolecules*, *8*, 1064–1068.
Shimada, J., Kaneko, H., Takada, T., Kitamura, S., & Kajiwara, K. (2000). Conformation of amylase in aqueous solution: small-angle X-ray scattering measurements and simulations. *Journal of Physical Chemistry B*, *104*(9), 2136–2147.
Wu, G., Tashiro, K., & Kobayashi, M. (1989). *Macromolecules*, *22*, 188–196.
Yamaguchi, Y., Nge, T. T., Takemura, A., Hori, N., & Ono, H. (2005). Characterization of uniaxially aligned chitin film by 2D FT-IR spectroscopy. *Biomacromolecules*, *6*, 1941–1947.